

Optical Relation of Plastically Deforming Polymer Solid

INTRODUCTION

Birefringent phenomena are examples of the electro-optical phenomena of deformable dielectrics. Many experimental studies of birefringence for polymers have been reported.¹⁻⁵ Theoretical birefringence has been reported for flowing polymer solutions (for example, polystyrene solutions) subjected to steady shear flow under the simplest possible relation (in which the stress tensor is equal to a constant multiple of the refractive index tensor plus an isotropic tensor).⁶

In this note, starting from the optical theory,⁷ the optical relation is theoretically deduced for plastically deforming polymer solid in creep and for proportional loading (namely, where uniform stress rate increases with time). The deduced optical relation is useful for nonsteady inelastic deformation as well as for steady inelastic deformation. Moreover, comparison of the deduced relation with the experimental results is discussed to ascertain the validity of the deduced relation. The optical relation of the first-order approximation gives good agreement with the actual observations obtained from the experiments in creep and for proportional loading tests using cellulose nitrate at 65°C. Cellulose nitrate is commonly used in photomechanics, especially in photoplasticity^{10,11} and in photoviscoplasticity.¹³

CONSTITUTIVE EQUATION OF PLASTICALLY DEFORMING POLYMER SOLID

For plastically deforming polymer solid used in the present study, the strain in an element of the polymer solid is proposed to consist of the Hookean elastic strain E_e , the plastic strain E_p , and the creep strain E_c . Here, the inelastic strain is defined as $E_i = E_p + E_c$. The elastic and the plastic strain components are expressed as¹²

$$(E_{ij})_e = \frac{S_{ij}}{2G} \quad (1)$$

and

$$(E_{ij})_p = \frac{S_{ij}}{2G} \left\{ \left(\frac{J_2}{k^2} \right)^n \right\} \quad (2)$$

where $S_{ij} = \sigma_{ij} - \frac{1}{3}\theta_{ij}\delta_{ij}$ is the deviatoric stress components of stress σ_{ij} ⁸; $J_2 = S_{ij}S_{ij}/2$ is the second invariant of the deviatoric stress tensor⁸; and G, k, n are material constants. With the components of principal stress σ_1, σ_2 , and σ_3 , J_2 is expressed as⁸

$$J_2 = \frac{1}{6} \{ (\sigma_1 - \sigma_2)^2 + (\sigma_2 - \sigma_3)^2 + (\sigma_3 - \sigma_1)^2 \} \quad (3)$$

The creep strain rate is approximately expressed as¹²

$$(\dot{E}_{ij})_c = B(t + s)^\alpha \exp(b J_2^{1/2}) (\partial J_2 / \partial \sigma_{ij}) \quad (4)$$

where t and s denote current time and material constant time and B, α , and b are material constants. The dot over $(E_{ij})_c$ in eq. (4) represents differentiation with respect to time.

In the present note, the stress state $\sigma_1 \neq \sigma_2 = \sigma_3$ is adopted. If the differences of principal stresses and of principal strains are denoted by $\Delta\sigma = \sigma_1 - \sigma_2$ and $\Delta E = E_1 - E_2$, respectively, the elastic and the inelastic strains become¹²

$$\Delta E_e = \frac{\Delta\sigma}{2G} \quad (5)$$

and

$$\Delta E_i = \frac{\Delta\sigma}{2G} \{ (\Delta\sigma/\sqrt{3}k)^{2n} \} + B \int_0^t (\tau + s)^\alpha \Delta\sigma \exp \left[\left(\frac{b}{\sqrt{3}} \right) \Delta\sigma \right] d\tau \quad (6)$$

The total strain is expressed as

$$\Delta E = \Delta E_e + \Delta E_i \quad (7)$$

This constitutive equation has been verified experimentally to be a good approximation for the plastically deforming polymer solid.^{12,13}

BASIC RELATIONS OF BIREFRINGENCE

The birefringent properties of a nonmagnetic solid depend on the index tensor η in the dielectric field.¹⁴ A solid after deformation is considered as an anisotropic one, and the electric induction \mathbf{D} and the electric field strength \mathbf{B} are related by the symmetrical tensor η , which is regarded as a function of the deformation state, as follows⁷:

$$\mathbf{B} = \eta \mathbf{D} \quad (8)$$

or

$$B_k = \eta_{kl} D_l$$

Suppose that an optically isotropic polymer plate is placed in the circular polarized field of a polariscope so that the face of the plate is normal to the axis of wave propagation. Consider a section of the index ellipsoid cut by the diametral plane perpendicular to the axis of wave propagation. The section is an ellipse, and it then has two principal directions, which are called the secondary principal axes. By choosing the secondary principal direction axes X_α ($\alpha = 1, 2$) as the coordinate axes, the ellipse is represented by

$$\eta_1(X_1)^2 + \eta_2(X_2)^2 = 1 \quad (9)$$

where η_1 and η_2 are the secondary principal values of η . The isochromatic fringe order per unit thickness in photomechanics is given by⁷

$$N = \omega \left(\frac{1}{V_2} - \frac{1}{V_1} \right) = \frac{\omega}{c} \left(\frac{1}{\sqrt{\eta_2}} - \frac{1}{\sqrt{\eta_1}} \right) \quad (10)$$

where ω , c , and $V_\alpha = c\sqrt{\eta_\alpha}$ ($\alpha = 1, 2$) are the frequency, the light velocity under vacuum, and the velocities of the polarized light, respectively.

Assuming that the solid is optically isotropic before deformation, the index tensor is rewritten as

$$\eta = \eta_0 \mathbf{I} + \tilde{\eta}$$

or

$$\eta_1 = \eta_0 + \tilde{\eta}_1, \quad \eta_2 = \eta_0 + \tilde{\eta}_2 \quad (11)$$

where η_0 and \mathbf{I} are the index coefficient and the unit tensor $\mathbf{I} = |\delta_{ij}|$, respectively. Equation (10) is approximately expressed for the principal values $\tilde{\eta}_1$ and $\tilde{\eta}_2$ as follows:

$$N = A(\tilde{\eta}_1 - \tilde{\eta}_2) \quad (12)$$

where $A = \omega/(2c \eta_0^{3/2})$.

The anisotropy that replaces the original optical isotropy is assumed to consist of the following two parts as mentioned in the previous section. One part corresponds to the elastic strain tensor \mathbf{E}_e with regard to the change of orientation of molecular chains. Another part corresponds to the inelastic strain tensor \mathbf{E}_i with regard to the permanent change of orientation of molecular chains appearing with the inelastic deformation of the solid and remaining even after vanishing of the stress.

When the axes of two tensors \mathbf{E}_e and \mathbf{E}_i coincide with each other, the index tensor $\tilde{\eta}$ is proposed as a function of the two tensors. The index tensor is given as

$$\tilde{\eta} = \mathbf{F}(\mathbf{E}_e, \mathbf{E}_i)$$

and the polynomial \mathbf{F} of two tensors can be represented as in the following form^{15,16}:

$$\begin{aligned} \tilde{\eta} = & a_0 \mathbf{I} + a_1 \mathbf{E}_e + a_2 \mathbf{E}_i + a_3 \mathbf{E}_e^2 + a_4 \mathbf{E}_i^2 \\ & + a_5 (\mathbf{E}_e \mathbf{E}_i + \mathbf{E}_i \mathbf{E}_e) + a_6 (\mathbf{E}_e^2 \mathbf{E}_i + \mathbf{E}_i \mathbf{E}_e^2) \\ & + a_7 (\mathbf{E}_e \mathbf{E}_i^2 + \mathbf{E}_i^2 \mathbf{E}_e) + a_8 (\mathbf{E}_e^2 \mathbf{E}_i^2 + \mathbf{E}_i^2 \mathbf{E}_e^2) \end{aligned} \quad (13)$$

where a_0, \dots, a_8 are coefficients composed of the invariants of \mathbf{E}_e and \mathbf{E}_i .

If the first-order approximation is adopted in eq. (13) for convenience of practical applications as an example, the index tensor is represented as

$$\tilde{\eta} = a_0\mathbf{I} + a_1\mathbf{E}_e + a_2\mathbf{E}_i$$

or

$$\tilde{\eta}_1 = a_0 + a_1E_{e1} + a_2E_{i1}, \quad \tilde{\eta}_2 = a_0 + a_1E_{e2} + a_2E_{i2} \quad (14)$$

where the subscripts 1 and 2 of the strain components denote the principal values of the strain tensor. The fringe order per unit thickness for the first-order approximation is derived from eq. (12) as follows:

$$N = C'_1(E_{e1} - E_{e2}) + C_2(E_{i1} - E_{i2}) \quad (15)$$

where C'_1 and C_2 are optical coefficients. In such a representation, as $\Delta E_e = (E_{e1} - E_{e2})$ is proportional to $\Delta\sigma = \sigma_1 - \sigma_2$ as shown in eq. (5), eq. (15) is expressed as

$$N = C_1(\Delta\sigma) + C_2(\Delta E_i) \quad (16)$$

where $\Delta E_i = E_{i1} - E_{i2}$.

EXPERIMENTAL

Tests were performed using the uniaxial specimens made of 6-mm-thick cellulose nitrate plate at 65°C in the axial tensile stress state: $\sigma_1 = \Delta\sigma$, $\sigma_2 = \sigma_3 = 0$. The experimental apparatus consists of three major systems, namely, an oil vessel with heater, a loading system, and instruments to record the load and deformation. The detailed descriptions of the specimen and the apparatus are shown in ref. 17. On a surface of each specimen, a square gauge mark was cut in a region of uniform stress. Axial elongation and cross contraction over the distance between the gauge marks cut on the specimen were measured to within 0.005 mm from photographs of the gauge marks using a magnifying projector. The difference of principal strains $\Delta E = E_1 - E_2$ was calculated in Green's strain system⁹ $E_\alpha = \epsilon_\alpha + (\epsilon_\alpha)^2/2$, where ϵ_α ($\alpha = 1, 2$) is conventional engineering strain. The accuracy of strain thus obtained is within about 2×10^{-4} . The fringe order of birefringence was measured by Tardy's method.¹⁸

Creep Tests

The creep tests were performed under the loading of axial tensile stress $\sigma_1 = \Delta\sigma$. Each load was applied so as to obtain constant values of $\Delta\sigma$ of 0.4, 0.6, 0.8, 1.0, and 1.15 kg/mm² at 65°C.

Figure 1 shows the experimental creep relation between the total strain $\Delta E = \Delta E_e + \Delta E_i$ and time for each value of $\Delta\sigma$. Each curve is plotted using the average values of three test results. The circle symbols and solid curves in Figure 2 show the relations between the fringe order per unit thickness N and time corresponding to the results shown in Figure 1.

Proportional Loading Tests

In the proportional loading tests under axial tensile stress, $\sigma_1 = \Delta\sigma$ increases linearly with time; $\Delta\sigma = \Delta\dot{\sigma}t$, where $\Delta\dot{\sigma}$ is constant stress rate and t denotes current time. Each load was applied so as to obtain constant rates $\Delta\dot{\sigma}$ of 0.025, 0.05, 0.1, and 0.2 kg/mm²/min at 65°C. The open circles in Figure 3 show the relations between $\Delta\sigma$ and the total strain ΔE for various values of $\Delta\dot{\sigma}$. Each curve is plotted by using average values of three test results. In Figure 3, as eq. (5), that is, $\Delta E_e(t) = \Delta\sigma(t)/(2G)$, approximates the relation in the range of small value of time t (namely, in the range of small value of $\Delta\sigma$), the value of $2G$ is found from the experimental result in this range. The gradient $2G$ ($= \Delta\sigma/\Delta E$) is shown by the chain line in Figure 3. By the chain line ΔE_i is divided into the elastic part ΔE_e and the inelastic part ΔE_i . Then, ΔE_i is remarkably influenced by the values of $\Delta\dot{\sigma}$. The solid circles in Figure 3 show the unloading relations between $\Delta\sigma$ and ΔE for $\Delta\dot{\sigma} = -0.1$ and -0.2 kg/mm²/min (namely, the stress rate decreases with time). As shown by the solid circles in Figure 3 at the early stage of the unloading process, the additional creep deformation continues to appear for the operating load even in the unloading process. These features of the inelastic deformation have been also recognized for another cellulose nitrate solid.¹³ The circle symbols and solid curves in Figure 4 show the relations between $\Delta\sigma$ and the fringe order per unit thickness N corresponding to the results shown in Figure 3.

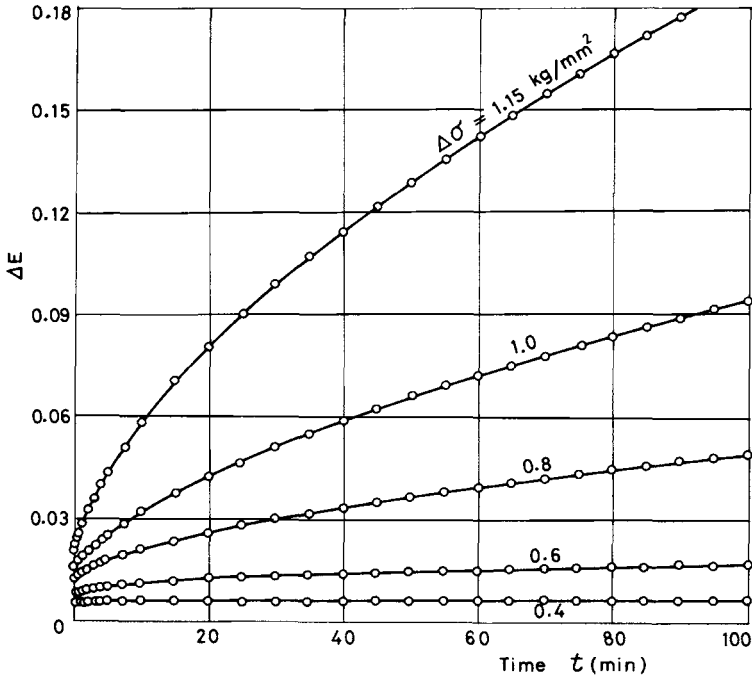


Fig. 1. Experimental creep relation between ΔE and time for each value of $\Delta\sigma$ at 65°C.

DISCUSSIONS AND CONCLUDING REMARKS

In Figure 4, as the inelastic strain ΔE_i may be negligibly small in the range of small value of time t (namely, in the range of small value of $\Delta\sigma$), the value of C_1 in eq. (16) is found from the experimental result in this range. The gradient $C_1 (= N/\Delta\sigma)$ is shown by the chain line in Figure 4. The value of C_2 is determined from the distance between abscissas of the chain line and the experimental curve in the range of the large value of $\Delta\sigma$ by using ΔE_i in Figure 3. The coefficients in eq. (16) were determined from the results for $\Delta\dot{\sigma} = 0.05$ kg/mm²/min shown in Figure 4, and they are as $C_1 = 0.23$ mm/kg and $C_2 = 1.7$ mm⁻¹.

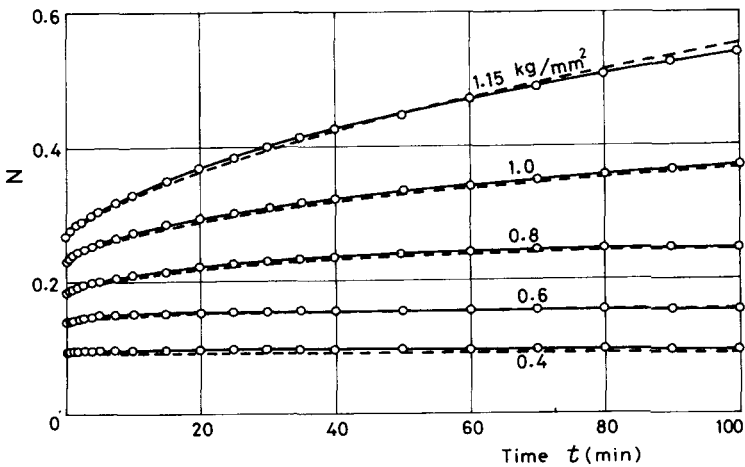


Fig. 2. Relation between fringe order per unit thickness N and time for each value of $\Delta\sigma$ in creep tests: (—○—) experiment; (---) eq. (16).

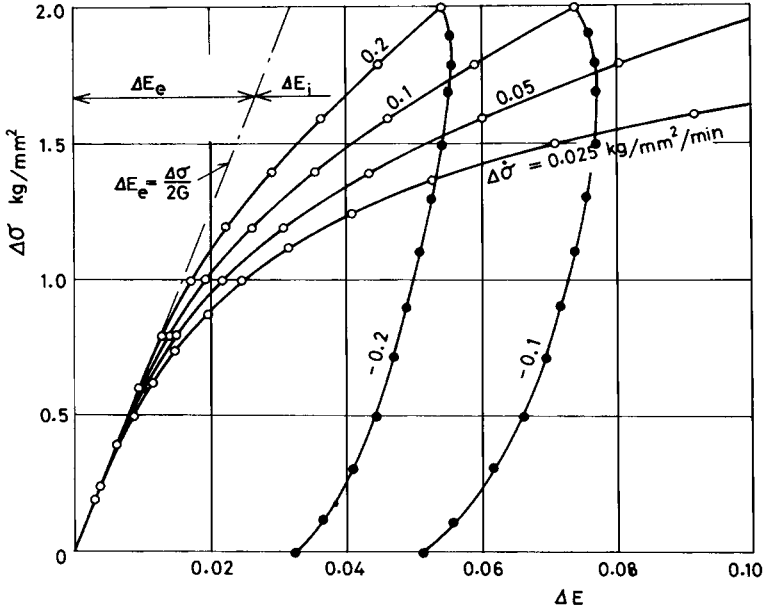


Fig. 3. Relations between $\Delta\sigma$ and ΔE for various values of $\Delta\dot{\sigma}$ in the proportional loading tests: (—○—) loading process; (—●—) unloading process.

The broken curves in Figure 4 were calculated from eq. (16) by using the values of C_1 and C_2 obtained and the corresponding values of ΔE_i in Figure 3. They agree well with the corresponding experimental results expressed by the solid curves for various values of the stress rate $\Delta\dot{\sigma}$ as shown in Figure 4.

Moreover, the broken curves in Figure 2 were calculated from eq. (16) by using the coefficients C_1 and C_2 obtained from the experiments in the proportional loading tests and by using the corre-

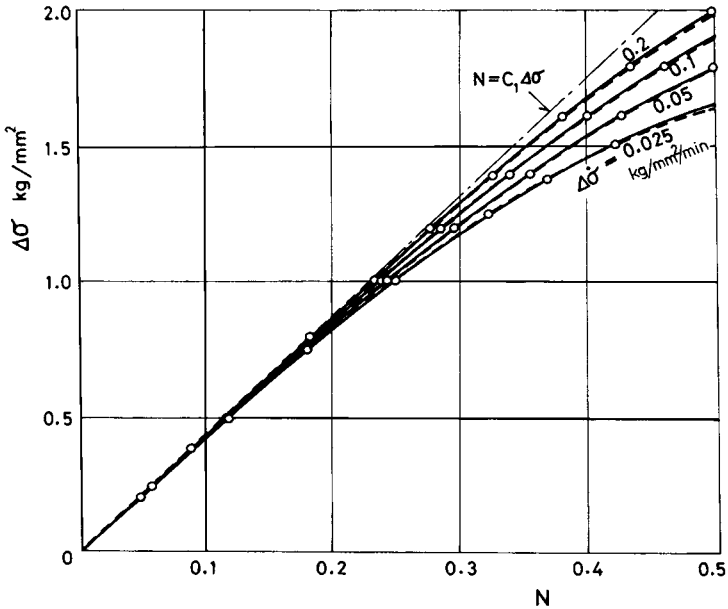


Fig. 4. Relations between $\Delta\sigma$ and the fringe order per unit thickness for various values of $\Delta\dot{\sigma}$: (—○—) experiment; (---) eq. (16).

sponding values of ΔE_i in Figure 1. In this case, the instantaneous strain at the instant of loading $t = 0$ in Figure 1 was assumed as the elastic strain ΔE_e , and the inelastic strain was assumed as $\Delta E_i = \Delta E - \Delta E_e$. The broken curves agree well with the corresponding experimental results expressed by the solid curves for various values of the stress $\Delta\sigma$ as shown in Figure 2.

From foregoing discussions, neglecting the small amount of error, it is concluded that the deduced optical relation (16) of the first-order approximation gives good agreement with the actual observations in creep and for proportional loading tests for plastically deforming polymer solid over the strain range $\Delta E = 0.15$, independent of values of stress $\Delta\sigma$ and of stress rate $\Delta\dot{\sigma}$.

References

1. A. Nishioka, J. Furukawa, and S. Yamashita, *J. Appl. Polym. Sci.*, **14**, 799 (1970).
2. M. Fukada, G. L. Wilkes, and R. S. Stein, *J. Polym. Sci. Part A-2*, **9**, 1417 (1971).
3. M. J. Folkes and A. Keller, *Polymer*, **12**, 222 (1971).
4. S. Raha and P. B. Bowden, *Polymer*, **13**, 174 (1972).
5. M. H. Liberman, Y. Abe, and P. J. Flory, *Macromolecules*, **5**, 550 (1972).
6. A. S. Lodge, *Nature*, **176**, 838 (1955).
7. A. Sommerferd, *Optics*, Academic, New York, 1957.
8. R. Hill, *The Mathematical Theory of Plasticity*, Clarendon, Oxford, 1950.
9. Y. C. Fung, *Foundations of Solid Mechanics*, Prentice-Hall, Englewood Cliffs, NJ, 1965.
10. M. M. Frocht, *Proceedings International Symposium on Photoelasticity*, Pergamon, New York, 1963.
11. J. Javornicky, *J. Strain Anal.* **3**, 33 (1967).
12. T. Nishitani, *J. Mater. Sci.*, **12**, 1185 (1977).
13. T. Nishitani, *Exp. Mechanics*, **19**, 102 (1979).
14. L. D. Landau and E. M. Lifschitz, *Electrodynamics of Continuous Media*, Pergamon, Oxford, 1960.
15. D. C. Leigh, *Nonlinear Continuum Mechanics*, McGraw-Hill, New York, 1968.
16. C. Truesdell and W. Noll, *The Nonlinear Field Theories of Mechanics*, Springer-Verlag, New York, 1965.
17. Y. Ohashi, *Br. J. Appl. Phys.*, **16**, 985 (1965).
18. R. B. Heywood, *Photoelasticity for Designers*, Pergamon, Oxford, 1969.

TADASHI NISHITANI
TOSHIHARU OHNISHI

Division of Applied Mechanics
Suzuka College of Technology
Suzuka, 510-02, Japan

Received June 15, 1978

Revised January 21, 1980